24th COBEM - 2017

24th ABCM International Congress of Mechanical Engineering
December 3-8, 2017, Curitiba, PR, Brazil

COBEM-2017-2419
ROBOTIC HAND CONTROLLED BY ELECTROMYOGRAPHIC SIGNALS

Pedro Agostinho Skrdlik
Rafael Silva Figueiredo
CEFET-RJ Undergraduate students of Control and Automation Engineering, Rio de Janeiro, Brasil
{pedroskrd, rafael.figueiredo1}@hotmail.com

Cristiano Souza Carvalho
Fabrício Lopes e Silva
Luciano Santos Constantim Raptopoulos
Waltencir dos Santos Andrade
NUPEM/CEFET-RJ - Mechatronics Research Center of the Federal Center for Technological Education Celso Suckow da Fonseca, Rio de Janeiro, Brasil
{cristiano.carvalho, fabricio.silva, luciano.raptopoulos, waltencir.andrade}@cefet-rj.br

Abstract. *In the current work an approach to the development of a prototype robotic hand controlled by myoelectric signals is presented. A three dimensional model of the prototype was created with the aid of additive manufacturing technology. After that, the and inverse kinematics and the dynamics of a human hand were modeled to achieve fully comprehension of the movements, permitting its analysis and adjustments in the model. The control system is based on artificial neural networks (ANNs). The reference to the control system is a set of electromyographic (EMG) signals, measured from the skin during the muscle contractions.*

Keywords: *hand kinematics, control system, artificial neural network, electromyographic signals.*

1. INTRODUCTION

The technological advances impelled studies in many areas of knowledge. The evolution in material sciences permitted the development of light weight structures, as well as, the development of compact and high capacity batteries. In the computational field, very powerful computers have been produced, making possible complex simulations and making effective sophisticated artificial intelligence algorithms.

The connection of the mentioned advances with the search for systems that mimics human body parts, specially the human hand, brought the possibility of designing efficient prosthetic hands. The technological advances permitted better autonomy to the device, making possible the usage of the prosthesis during a longer time, without need to recharge, as well as, the production of prosthesis with lower cost and better quality. Sensors that improve acquired signals and new control strategies that optimized the movements, permitted even more quality to the prosthetics behavior. The digital and electronic development also made the adaptation and performance of prosthesis much better.

The development of artificial intelligence methodologies and algorithms, like the artificial neural networks (ANN), permitted to simulate specific behavior of human brain. It can present high complexity, nonlinearities and also can process data in a parallel pattern (Haykin, 1999). In this way, they can accomplish difficult tasks with relative easiness, making it behave more as a human hand. All this evolution make the prosthesis become even more sophisticated, accessible and functional.

2. PROSTHETIC HAND

In order to develop a bio-inspired prosthetic hand in this work, some factors were evaluated, using the following methodology. At first, the anthropometry of a hand was studied to give anthropomorphic characteristics to the prosthetic hand. Secondly, the actuation of the system together with its mechanical properties were investigated. And finally, the activation for the prosthesis movement was investigated and processed in a way to use it as a signal to drive the strategy of actuation.

2.1 ANTHROPOMETRY

Anthropometry is the part of the human science that study body metrics, mainly size and format (Rodriguez-Añez, 2001). An anthropometric study must be developed according to specific standards in order to keep some pattern in the measurement procedure (Perini *et al.*, 2005). In this work, the lengths presented in Fig. 1(a), Fig. 1(b) and Fig. 1(c) were used to determine the lengths of the proposed prosthetic hand.

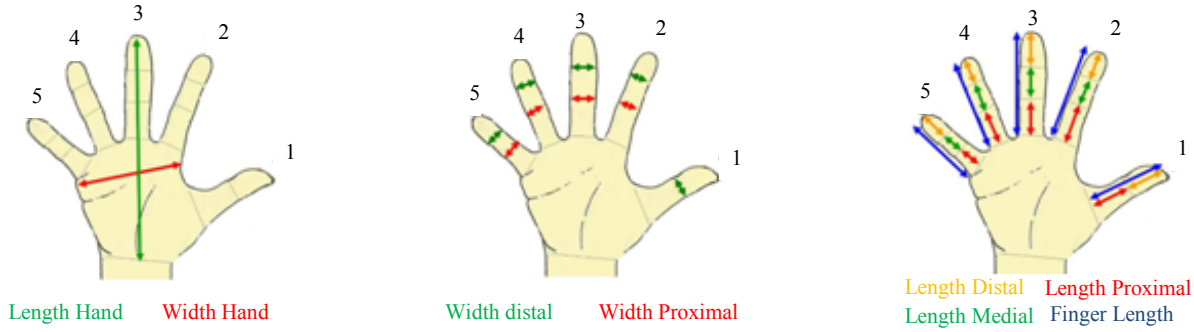

(a) (b) (c)

Figure 1: Measured dimensions.

Table 1: Results of anthropomorphic measures

		golden	Fotogrametry	Pachimetry
			Media (d.p.)	
1	Palm width	97.250	95.510 (± 0.11)	95.446 (± 0.38)
2	Proximal width of the 2nd finger	23.070	20.550 (± 0.13)	22.750 (± 0.14)
3	Distal width of the 2nd finger	19.810	17.456 (± 0.10)	19.482 (± 0.04)
4	Proximal width of the 3º finger	23.460	22.080 (± 0.13)	23.392 (± 0.08)
5	Distal width of the 3rd finger	19.730	18.156 (± 0.11)	19.562 (± 0.21)
6	Proximal width of the 4th finger	22.290	21.152 (± 0.11)	21.982 (± 0.16)
7	Distal width of the 4th finger	18.640	18.070 (± 0.11)	18.606 (± 0.07)
8	Proximal width of the 5th finger	18.980	17.408 (± 0.11)	18.416 (± 0.11)
9	Distal width of the 5th finger	17.500	16.286 (± 0.11)	17.232 (± 0.14)
10	Total length of the hand	189.420	186.900 (± 0.14)	188.490 (± 0.91)
11	Total length of the 1st finger	65.280	63.238 (± 0.12)	65.650 (± 1.47)
12	Proximal length of the 1st finger	30.070	30.588 (± 0.13)	30.868 (± 0.57)
13	Distal length of the 1st finger	35.800	32.864 (± 0.10)	35.822 (± 1.10)
14	Total length of the 2nd finger	73.500	73.714 (± 0.12)	73.110 (± 1.21)
15	Proximal length of the 2nd finger	25.640	26.294 (± 0.12)	25.840 (± 0.41)
16	Medial length of the 2nd finger	22.330	22.258 (± 0.10)	22.466 (± 1.04)
17	Distal length of the 2nd finger	25.620	25.292 (± 0.09)	25.506 (± 0.59)
18	Total length of the 3rd finger	80.850	79.424 (± 0.40)	80.198 (± 0.91)
19	Proximal length of the 3rd finger	28.160	27.360 (± 0.12)	27.776 (± 0.66)
20	Medial length of the 3rd finger	26.060	27.650 (± 0.11)	26.338 (± 0.48)
21	Distal length of the 3rd finger	26.620	26.056 (± 0.09)	25.936 (± 0.84)
22	Total length of the 4th finger	76.850	76.682 (± 0.09)	76.120 (± 0.60)
23	Proximal length of the 4th finger	23.520	23.406 (± 0.11)	23.848 (± 0.36)
24	Medial length of the 4th finger	25.740	26.306 (± 0.10)	25.976 (± 0.29)
25	Distal length of the 4th finger	27.610	26.924 (± 0.28)	27.518 (± 1.85)
26	Total length of the 5th finger	65.310	63.774 (± 0.32)	64.110 (± 0.58)
27	Proximal length of the 5th finger	21.720	21.800 (± 0.12)	22.750 (± 0.39)
28	Medial length of the 5th finger	18.460	18.106 (± 0.11)	18.022 (± 0.33)
29	Distal length of the 5th finger	25.150	24.186 (± 0.09)	24.064 (± 0.36)

The measurements were guided through three different methods, as proposed by Klein (2009), (1) photogrametry,

(2) coordinates measure machine (CMM) and (3) pachymetry. Individuals were randomly selected in order to generate average dimensions for each part of a hand. The chosen population was composed by people over 18 years old, of any ethnicity or occupation, with five fingers at each hand and that theirs hands where at nice conditions. A total of 1100 men and 1100 women had their hands measured, ensuring an error by sample about 3%, as presented in Tab 1. Using the acquired data, the ratio between each length of the hand and its palm width is calculated and consequently, the lengths of each segment of the hand are obtained.

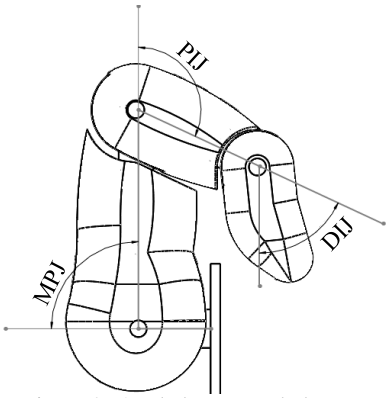

Figure 2: Angle between phalanges.

In addition to a study complaining the dimensions of each part of the hand, the rotation angle for each joint must be observed. In that case, the angles minor than zero are neglected. For the closed hand, the adopted limit angle for each joint are 65° to distal interphalangic joint (DIJ), 115° to proximal interfalangic joint (PIJ) and 90° to metacarpal phalangic joint (MPJ), identified at Fig 2 as proposed by (Kosmashi, 2017).

In order to create an adequate prototype, a three dimensional model (Schmit, 2003) was adopted but it wasn't prepared to be printed or be used as a prosthesis. some adaptations were necessary. Images of the prototype model are presented in Fig. 3 and Fig. 4

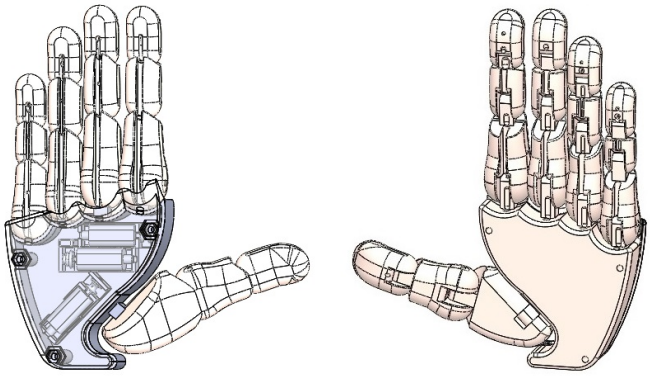
Figure 3: Hand model.

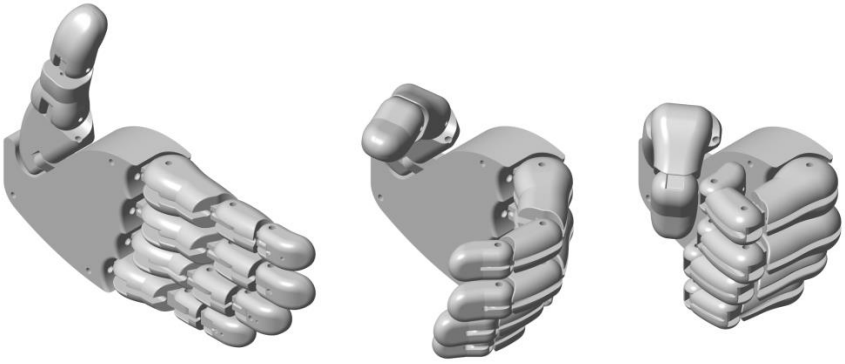
Figure 4: Movement of the hand.

2.2 MATERIAL

Additive manufacturing (AM) is a process of joining materials to make objects from 3D model data, usually layer-upon-layer, as opposed to subtractive manufacturing methodologies (ASTM:F2792, 2015). According to the ASTM Standard Organization, the AM methodology can be categorized by different processes, (1) Binder Jetting (BJ), an additive manufacturing process in which a liquid bonding agent is selectively deposited to join powder materials; (2) fused deposition modeling (FDM), a material extrusion process used to make thermoplastic parts through heated extrusion and deposition of materials layer by layer; (3) material jetting (MJ), process in which droplets of build material, including photo-polymer and wax, are selectively deposited; (4) powder bed fusion (PBF), process in which thermal energy selectively fuses regions of a powder bed; and (5) vat photo-polymerization, process in which liquid photo-polymer in a vat is selectively cured by light-activated polymerization, it can be done by laser (STL - stereolithography) or even by another light type (ultra-violet, for example).

The proposed prototype was manufactured using the FDM process, to which two different materials are available. Usually, PLA and ABS are the most common materials applied in such kind of manufacturing. Although acrylonitrile butadiene styrene (ABS) and polylactic acid (PLA) are materials that have melting temperatures low enough to use in melt extrusion outside of a dedicated facility, for both the melting temperatures are high enough for prints to retain their shape at average use temperatures. Therefore, the choice for an adequate material depends on the functionality of the object to be produced.

In order to chose the most adequate material the basic tensile strength and elastic modulus of printed components were used. According to Tymrak *et al.* (2014), in realistic environment conditions for standard users 3D printers, the ABS material presents an average tensile strength of $28.5MPa$ and an average elastic modulus of $1807MPa$. For the same conditions, the PLA material presents an average tensile strength of $56.6MPa$ and an average elastic modulus of $3368MPa$.

In order to verify the proposed system, a initial test was performed with PLA material. Some parts of the proposed model were printed to assemble one of the fingers of the proposed hand. As presented in Fig. 6, the used method is totally suitable to produce the proposed device. As presented in Fig. 5 and Fig. 6, the used method is totally suitable to produce the proposed device.

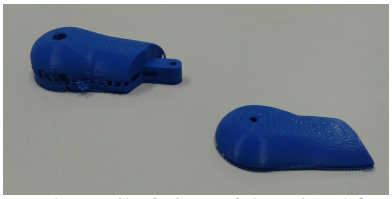

Figure 5: Detail of piece of the printed finger.

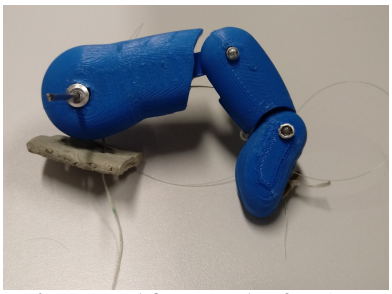

Figure 6: Mounted finger made of PLA material.

3. MATHEMATICAL MODELING

For the development of a robotic hand is essential to create a mathematic model that represents the system. This model permits to locate each part of the prototype, to plan the mechanisms that move fingers and to calculate the joint torques for dimensioning actuators.

3.1 FORWARD KINEMATICS

The Forward kinematics permits to know the position of each part of the system, according to the joint angles, the geometry of each part and reference systems. With this informations it is important to localize the extremities of each finger and the center of mass of each part or linkage of the system. The position of any point of the proposed system is

calculated using transformation matrices, as presented in Eq. 1.

$$\begin{bmatrix} O_{3x3} & P_{3x1} \\ p_{1x3} & e_{1x1} \end{bmatrix} = \begin{bmatrix} n_x & s_x & a_x & p_x \\ n_y & s_y & a_y & p_y \\ n_z & s_z & a_z & p_z \\ 0 & 0 & 0 & 1 \end{bmatrix} \tag{1}$$

In this work, the prosthesis behavior was investigated with basis on the human hand movement. To permit a simplified study of the proposed system, an individual study was conducted for each finger, once they have a similar structure. The human finger may be compared to a system composed by a open chain with three linkages, the phalanges proximal (l_{x1}), medial (l_{x2}) and distal (l_{x3}). In this notation "x" represents each finger, for example, the medial phalange of the ring finger is named l_{32}, once it is the second phalange of the third finger. The finger joints were modeled as three revolution joints, in which the rotation around Y axis corresponds to extension and flexion of the finger, besides a fourth rotation at Z axis on the first joint, perpendicularly to the hands palm that corresponds to the adduction and abduction of the finger. The revolution joints are named respectively as metacarpal phalangic joint (MPJ), proximal interphalangical joint (PIJ) and distal interphalangical joint (DIJ), remembering that in the human MPJ there are two rotations. The angles at model are named as θ_{x1}, θ_{x2} and θ_{x3}, as well as the notation used for the linkages. This rotations are around Y axis. In the model the rotation around the Z_0 axis is considered to be always zero.

The MFJ is the origin of the inertial reference system, and when all joints angles are equal to zero, the whole finger is positioned parallel to the X axis of the inertial system. In that way, all three rotations are performed with respect to the Y axis, as illustrated in Fig 7. The lateral movement is modeled by a rotation of this subsystem with respect to the inertial Z axis.

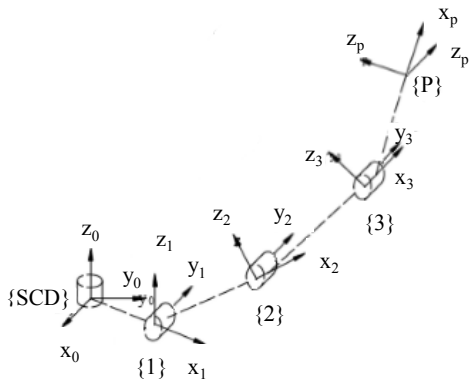

Figure 7: Finger coordinate system.

The math representation using matrix is shown in Eq. 2,

$$\begin{bmatrix} cos(\theta_{x1}) & -sin(\theta_{x1}) & 0 & 0 \\ sin(\theta_{x1}) & cos(\theta_{x1}) & 0 & 0 \\ 0 & 0 & 1 & 0 \\ 0 & 0 & 0 & 1 \end{bmatrix} \cdot \begin{bmatrix} 1 & 0 & 0 & l_{x1} \\ 0 & 1 & 0 & 0 \\ 0 & 0 & 1 & 0 \\ 0 & 0 & 0 & 1 \end{bmatrix} \cdot \begin{bmatrix} cos(\theta_{x2}) & -sin(\theta_{x2}) & 0 & 0 \\ sin(\theta_{x2}) & cos(\theta_{x2}) & 0 & 0 \\ 0 & 0 & 1 & 0 \\ 0 & 0 & 0 & 1 \end{bmatrix} \cdot$$

$$\begin{bmatrix} 1 & 0 & 0 & l_{x2} \\ 0 & 1 & 0 & 0 \\ 0 & 0 & 1 & 0 \\ 0 & 0 & 0 & 1 \end{bmatrix} \cdot \begin{bmatrix} cos(\theta_{x3}) & -sin(\theta_{x3}) & 0 & 0 \\ sin(\theta_{x3}) & cos(\theta_{x3}) & 0 & 0 \\ 0 & 0 & 1 & 0 \\ 0 & 0 & 0 & 1 \end{bmatrix} \cdot \begin{bmatrix} 1 & 0 & 0 & l_{x3} \\ 0 & 1 & 0 & 0 \\ 0 & 0 & 1 & 0 \\ 0 & 0 & 0 & 1 \end{bmatrix} = \tag{2}$$

$$\begin{bmatrix} cos(tx) & -sin(tx) & 0 & l_{x1} \cdot cos(\theta_{x1}) + l_{x2} \cdot cos(\theta_{x1} + \theta_{x2}) + l_{x3} \cdot cos(\theta_{x1} + \theta_{x2} + \theta_{x3}) \\ sin(tx) & cos(tx) & 0 & l_{x1} \cdot sin(\theta_{x1}) + l_{x2} \cdot sin(\theta_{x1} + \theta_{x2}) + l_{x3} \cdot sin(\theta_{x1} + \theta_{x2} + \theta_{x3}) \\ 0 & 0 & 1 & 0 \\ 0 & 0 & 0 & 1 \end{bmatrix}$$

With this individual analysis a new inertial reference was considered at the center of the pulse. In that way, each finger presents a location to its MPJ. The distance from this joint to the new origin is represented by a translation matrix,

pre-multiplying the matrix of transformation of each finger.

$$\begin{bmatrix} cos(tx) & -sin(tx) & 0 & l_{x1}\cdot cos(\theta_{x1}) + l_{x2}\cdot cos(\theta_{x1}+\theta_{x2}) + l_{x3}\cdot cos(\theta_{x1}+\theta_{x2}+\theta_{x3}) \\ sin(tx) & cos(tx) & 0 & l_{x1}\cdot sin(\theta_{x1}) + l_{x2}\cdot sin(\theta_{x1}+\theta_{x2}) + l_{x3}\cdot sin(\theta_{x1}+\theta_{x2}+\theta_{x3}) \\ 0 & 0 & 1 & 0 \\ 0 & 0 & 0 & 1 \end{bmatrix} \cdot \begin{bmatrix} 1 & 0 & 0 & px \\ 0 & 1 & 0 & 0 \\ 0 & 0 & 1 & pz \\ 0 & 0 & 0 & 1 \end{bmatrix} = \tag{3}$$

$$\begin{bmatrix} cos(tx) & -sin(tx) & 0 & px + l_{x1}\cdot cos(\theta_{x1}) + l_{x2}\cdot cos(\theta_{x1}+\theta_{x2}) + l_{x3}\cdot cos(\theta_{x1}+\theta_{x2}+\theta_{x3}) \\ sin(tx) & cos(tx) & 0 & l_{x1}\cdot sin(\theta_{x1}) + l_{x2}\cdot sin(\theta_{x1}+\theta_{x2}) + l_{x3}\cdot sin(\theta_{x1}+\theta_{x2}+\theta_{x3}) \\ 0 & 0 & 1 & pz \\ 0 & 0 & 0 & 1 \end{bmatrix}$$

For the thumb structure, a very similar modeling was used. To simplify the model and the actuation, the adduction and abduction movement were neglected. For the thumb, in the calculation, the transformation matrix must be pre-multiplied by a rotation matrix that changes its orientation, different from the other ones, that are aligned with the inertial X axis. So, the prosthesis is able to smoothly perform the grasp movement when commanded to do so. Then, this matrix is pre-multiplied by the translation matrix, resulting in the transformation matrix of the finger tip with respect to the wrist, which is not considered in this study.

As the actuation of each finger will be conducted by tensioning cables, the variation of the released cable length for flexion and extension were calculated (Tab 2).

Table 2: Calculation of cable length (flexion and extension).

Finger	Flexion cable (mm)	Extension cable (mm)	Extension pulley diameter (mm)	Flexion pulley diameter (mm)
index	42,4	30,5	6,8	4,9
midle	43,5	31,3	6,9	5,0
ring	37,0	29,8	5,9	4,8
little	29,5	30,5	4,7	4,9

It is perceptible that the flexion variations are approximately the same for all fingers because of its geometry. All dimensions are in millimeter and these dimensions variation were calculated comparing the hand closed and opened. The pulley diameter was calculated to permit the prosthesis to close the hand on a half second using the maximum velocity of the motor ($320RPM$). The calculated length was performed considering a diameter of $3mm$ for the motor shaft, what limits the pulley diameter.

A correct diameter is important to avoid fingers closing with different velocities and, when more than one cable is fixed at the same pulley structure, the cables do not receive an inappropriate traction.

3.2 DYNAMICS

In the dynamical model of the hand, phalanges and hands palm were modeled as rigid bodies. As the system corresponds to open kinematic chains, the Lagrange method for those kind of configuration was used. To represent each articulation of the hand, revolution joints were adopted. Therefore, the adduction and abduction movements were neglected. In the adopted model, were not considered the dissipation through friction in the joints.

In order to calculate the dynamics of the prosthetic hand, the used inertial parameters were obtained through Solidworks®, while the Matlab® and Simulink® were used in the numerical solution of the model. The torque is calculated as the Eq. 4.

$$\tau = [M(q)].\ddot{q} + H(q,\dot{q}) + G(q) \tag{4}$$

In which τ is the vector of torques at the joints; $[M(q)]$ is the mass matrix of the system, $H(q,\dot{q})$ is the vector of terms related to effects of Coriolis and centrifugal; $G(q)$ is the term for torques relating to gravity; and $\ddot{q}$ is the acceleration vector of joints.

4. SYNCHRONIZATION SYSTEM BASED ON ARTIFICIAL INTELLIGENCE

Electromyographic signals (EMG) are originated from the recruitment of motor units (MU). Neurologically the motor unit consists of a synaptic junction in the ventral root of the spinal cord, a motor axon, and a motor end plate in the muscle

fibers (Winter, 2009). According to the *size principle*, proposed by Hennemann (1957), these motor units are recruited sequentially starting from the smaller MU and finishing with the bigger one (Winter, 2009). Each recruited MU presents an electric signal called action potential, and this signal's frequency increases with the raise of muscular tension. EMG signals are the algebraic summation of each motor unit's action potential.

In order to capture myoelectric signals, it was developed a technique called electromyography. The surface electromyography (sEMG) consists in the placement of electrodes in the skin's surface in the vicinity of the desired muscle. It is a quite simple and non-invasive technique. The equipment chosen to capture the signals is the BTS FreeEMG 1000. Its wireless EMG probes send the measurements to the receiving unit, and the information is read by the EMG Analyzer, software sold along with the equipment. This software is not capable of exporting data as soon as the readings are made, so the study is being conduced off-line in this initial approach (FREEEMG, 2008).

However, electromyographic signals must first be preprocessed due to the fact that they are affected by noise sources and artifact. To remove its influence on the EMG signals, it is necessary that they pass through some filters. It was already proved that most of the power of these signals is located between 20 and 200 Hz (De Luca *et al.*, 2010). The power line generates noise components at 60 Hz, while artifacts act at low frequencies, generally bellow 20 Hz. This way, a band-reject filter with range equal to 59-61 Hz, a high-pass filter with corner frequency equal to 20Hz and a low-pass filter with corner frequency equal to 200 Hz were created in Matlab® accomplish do this task.

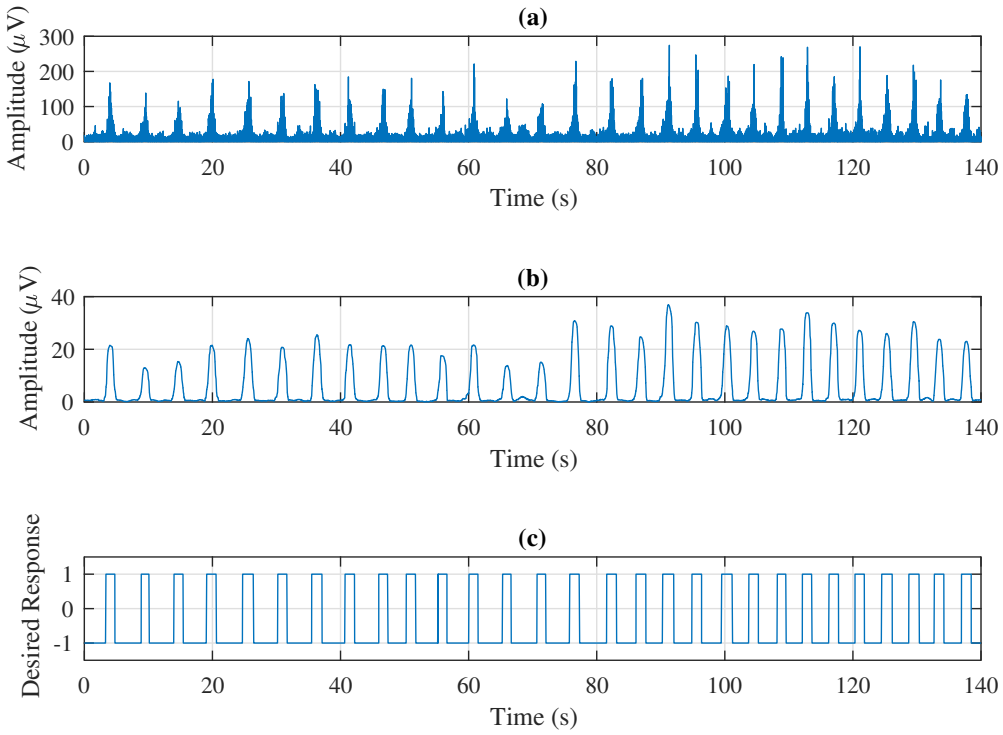

Figure 8: The filtered signal's absolute value (a), its root-mean-square envelope (b) and the signal describing the complete flexion (1) or complete extension (-1) of each finger (c).

After that, the absolute value is calculated for each filtered signal and then, the root-mean-square envelope of each one is calculated. Some tests were made, at the current stage of the study, to determine an adequate way to determine the fingers' complete flexion/extension periods based on the myoelectric signals' envelopes, as can be seen in Fig. 8. All this pre-processing steps were conduced in Matlab®.

Once the signals are conditioned, an artificial neural network (ANN) is created and trained, also in Matlab®. To train a neural network means present input samples and the correspondent target output. This is called supervised training. The architecture chosen for this initial study is a Multilayer Perceptron (MLP), a kind of multiple layer feed-forward network, composed by a single hidden layer, which is formed by twenty artificial neurons, and an output layer formed by a single artificial neuron. The neurons in the hidden layer have the hiperbolic tangent as its activation function, while the output layer's neuron have the linear function in this role.

As long as the neural network's training process is finished, it is ready to enter operation mode in order to validate its behavior. In operation mode, only input signals (the envelope of the EMG signals) are presented to the ANN, and it

is expected a correct classification of the finger's flexion (logical level +1) and extension periods (logical level -1). This stage is also conduced in Matlab®.

At the study's current step, three movements are being analyzed: the flexion/extension of the index finger, of the group formed by middle, ring and pinky fingers and of all the fingers together. The electrodes were positioned in the forearm, next to the elbow. This placement is justified by the fact that the prosthesis is being designed taking in account not only hand amputees, but also people who have lost part of the forearm.

4.1 MOTORS AND ELECTRONICS

The system determines the rotation of the motor for each finger or if it will need to stay static. If the signal is 0, the motor will keep static and locked, waiting for signal -1 to be actioned at anticlockwise or 1 to rotate at clockwise. After the decision, the micro controller send an output signal using pulse width modulation (PWM) to control the motor velocity. With this signal the power drive (H bridge), mounted with integrated circuit L293, activates the motor at clockwise or anticlockwise.

In the Figure 9, a flow chart is presented in order to explain how the system works from the signal 1 , 0 or -1, according to acquired EMG signal until motor activation. It's important to emphasize that this system is repeated three times identically to activate each direct current motor.

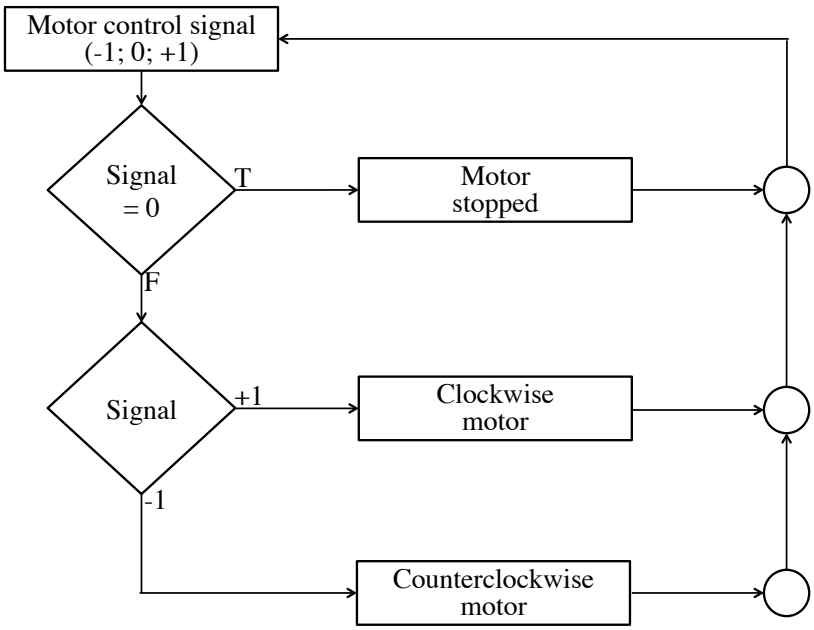

Figure 9: Flow chart of signals to the motors

4.2 ACTUATION AND UNDERACTUATION

Some forms of actuation as hydraulic, pneumatic or shape memory alloy (SMA) were cogitated to move the fingers due to its similarity with the muscular behavior, reducing its length when activated. Hydraulic or a pneumatic system need a pump or a compressor that are much bigger and heavier than a battery. The difficulty with the SMA is that after actuation and assumed the contracted form, it spends long time dissipate heat and to return to the original condition. Therefore, electric motors were elected the best choice for the actuation of each finger, considering price, control easiness and variety of options.

The power transmission through cables was chosen due to the similarity of them with human tendons. After research about physiology where chosen the best points for insertion of the cables on the prosthesis and were included on the model a local where this cable can be fixed. Besides on the human body the muscles that make the movement of the fingers are located on the forearm, was decided to put the motors on the hand. It was considered because if the motor stay out the hand, people that lost only the hand won't can use the prosthesis, because it would have an compartment were is placed the user forearm.

The idea of using underactuated joints on the project is to spend less energy, increasing the autonomy of the prosthesis. Moreover, it reduces the cost of that because will reduce the quantity necessary motors. When less actuators are used some movements that a human hand can do will be lost, once an unique motor will make the function of many muscles that normally works independently.

The achievement of the three joints of the finger is intuitive because it is something that happens naturally at human

body. The flexor and extensor tendon are inserted at the basis of the distal phalanges and are actuated by muscles at forearm, and for this reasons, for some individuals some movements are difficult to perform. Very unusual, and for ones, impossible, the flexion of any phalangical joint independently was considered usefulness, a motor for each piece of the finger will not cause a relevant functional lost.

The four fingers move together almost as frequently as do all combinations of fewer than four fingers (17% compared to 20%, respectively). It is relatively rare for one finger to move in isolation (7%) and more than half of such movements (68%) involve the thumb. In addition, of the 6% of movements, which involved the thumb and a single finger, almost half (47%) of such movements involved the index finger. This special relationship between the thumb and index finger is suggestive of the precision tip pinch grip. These patterns of movements show that the hand, most frequently, moves as a unit and that isolated movements of individual digits are rare (Ingram *et al.*, 2008). For this reasons was verified that the actuation of four fingers with one motor each, would be advantageous. In this work, only middle, ring and little finger are actuated by one motor to preserve pinch movement and click movement.

5. RESULTS AND DISCUSSIONS

The current methodology resulted in satisfactory results for the grasp movement, which was studied using the EMG signal from the *left extensor carpi ulnaris*. The flexion/extension periods are well distinct, as illustrated in Fig. 10. However, for the other two movements, the response presents some misclassification, as seen in Fig. 11 and Fig. 12.

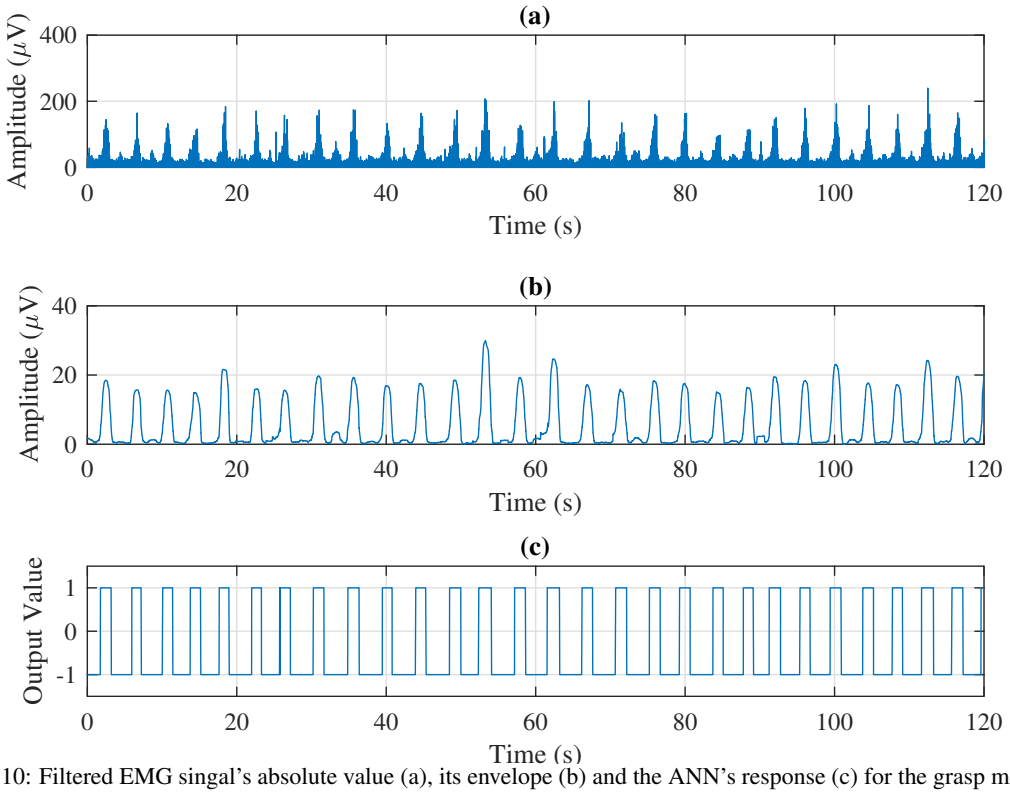

Figure 10: Filtered EMG singal's absolute value (a), its envelope (b) and the ANN's response (c) for the grasp movement.

The index flexion/extension movement was studied through a nonlinear combination of the EMG signals measured from the *left palmaris longus* and from the *left extensor carpi ulnaris*, while the study of the flexion/extension movement from the group formed by middle, ring and little fingers was carried using these two EMG signals at the same time but separately.

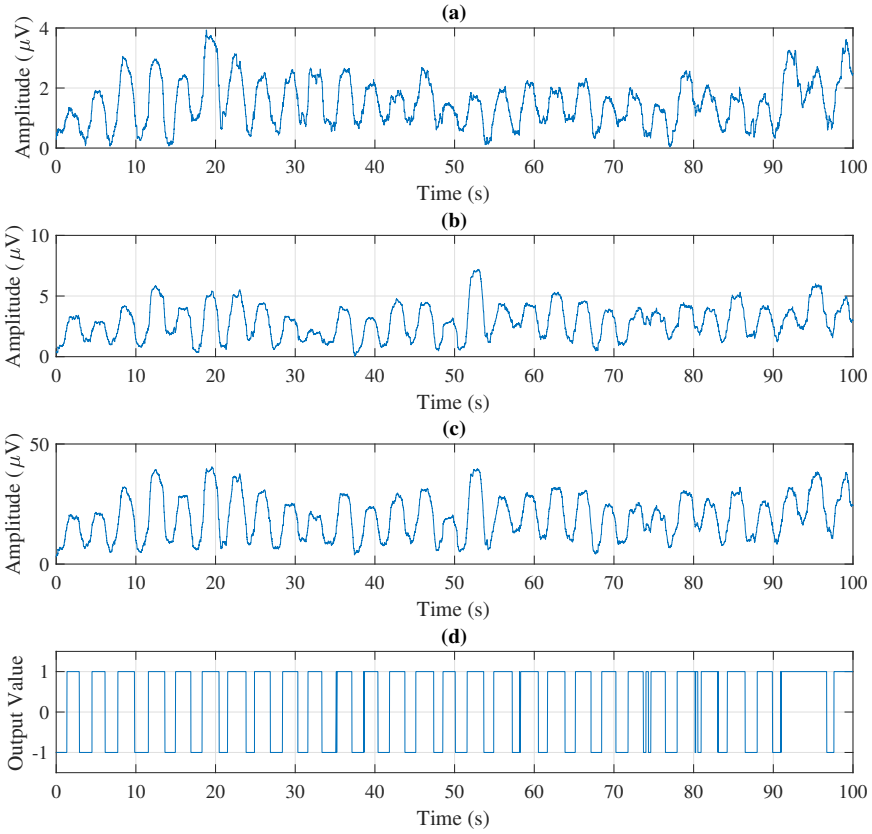

Figure 11: Filtered EMG singals' envelopes (a and b), its nonlinear combination (c) and the ANN's response (d) for the index flexion/extension movement.

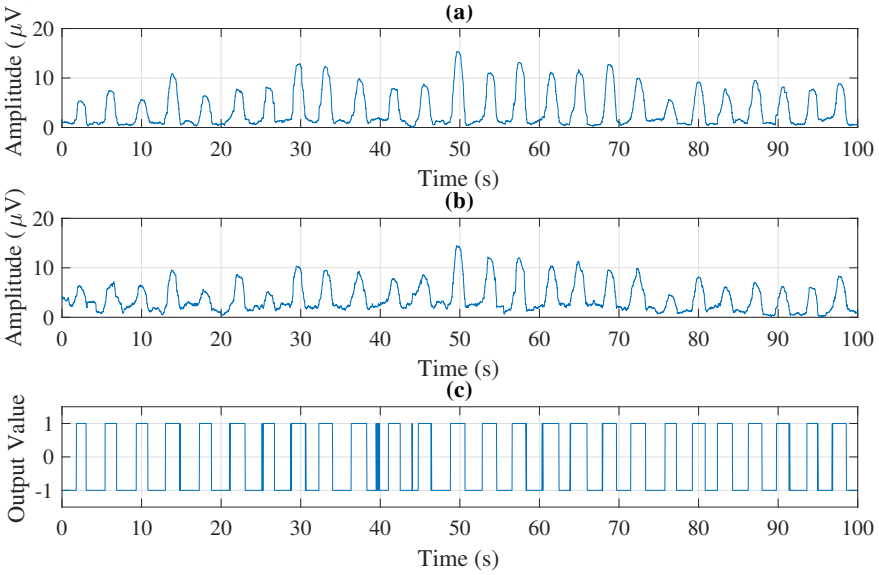

Figure 12: Filtered EMG singals' envelopes (a and b) and the ANN's response (c) for the flexion/extension movement of the group formed by middle, ring and pinky fingers.

It can be inferred that this behavior is related to a problem in the current methodology applied to these movements or related to the positioning of the EMG probes. Besides, as long as this work has just reached this step, it was not measured EMG signals from a proper number of subjects. This initial approach was made with the measurements from one of the authors. In the near future, it will be created a database with myoelectric signals from several volunteers, in order to extract general information carried by EMG signals related to the fingers' kinematics and dynamics. In that way, in future works, the ANNs will not determine only the complete flexion/extension for each finger. But also, the neural network's

response will represent the angle assumed by the fingers' joints. In other words, it will be possible for the prosthesis to assume intermediate positions between complete flexion and extension.

In order to analyze the dynamic behavior of the model, cubic trajectories were established for the flexion movement of the fingers. The trajectories of each joint were synchronized by the neural network developed for this work. The results from the dynamics of each joint are shown in Fig. 13.

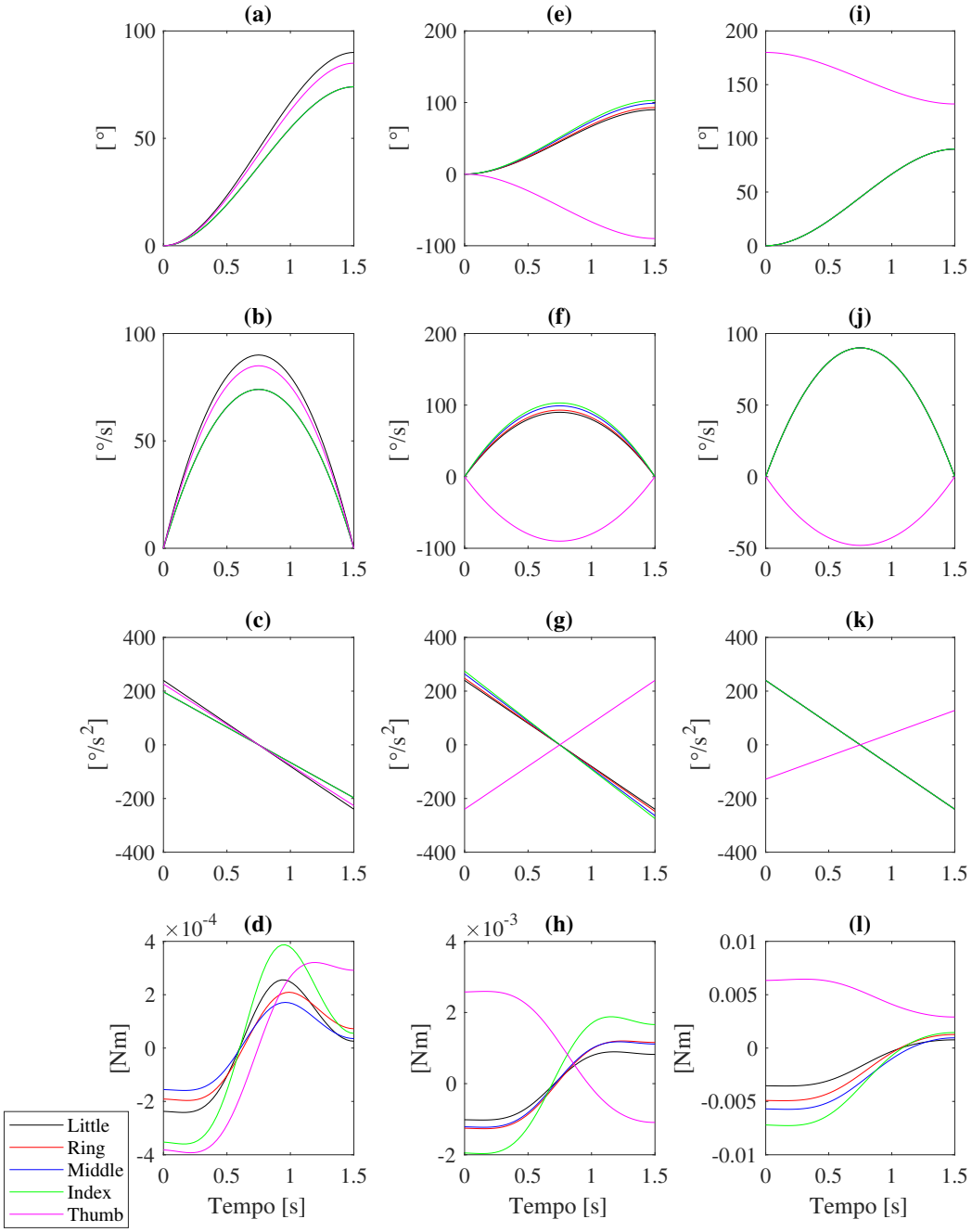

Figure 13: Dynamical result of the simulation: (a, b, c and d) are the results for DIJ, (e, f, g and h) are the results for PIJ and (i, j, k and l) are the results for MPJ.

6. CONCLUSION

The proposed prosthetic hand was planned to be produced through one of the most common additive manufacturing technologies. The Fused Deposition Modeling (FDM) works laying down in layers materials that come from coiled plastic filaments. The development of such kind of technology permitted the development of products in very complex shapes and in a very easy way. The popularization of those equipments have impacted the manufacturing processes. Although very sophisticated materials are already available, the adopted methodology took into consideration the use of accessible material.

In this work the initial study of a bio-inspired under actuated prosthesis in the human hand was presented. The dynamical study was performed in the open kinematic chain of the mechanism, being presented to the kinematic graphs and the torques in each one of the articulations modeled. From the motion activation layer, defined by a neural network designed to recognize the start and end times of each cycle of opening or closing the hand from the EMG signal measurement. In this stage of the work the desired kinematics for the movement of each joint was parameterized as a cubic order trajectory.

As the torque calculated to move DIJ was the smaller and the MIJ is the bigger, when the motor tract the cable, first the DIJ will rotate and subsequently PIJ and MIJ. To correct the movement and turn it more natural is pretend to put elastics differently tract to equilibrate the torques at joints and make a better movement of the finger.

7. ACKNOWLEDGEMENTS

The present work was partially supported by the CNPq Council, FINEP, DIPPG/CEFET-RJ and FAPERJ.

8. REFERENCES

ASTM:F2792, 2015. "Standard terminology for additive manufacturing technologies". URL `https://www.astm.org/Standards/F2792.htm`.

De Luca, C.J., Gilmore, L.D., Kuznetsov, M. and Roy, S.H., 2010. "Filtering the surface emg signal: Movement artifact and baseline noise contamination". *Journal of biomechanics*, Vol. 43, No. 8, pp. 1573–1579.

FREEEMG, B., 2008. *Manual de insssals*. BTS Bioengineering, 1st edition. URL `http://www.biomech.uottawa.ca/english/teaching/apa6905/lectures/2012/freeemg.pdf`.

Haykin, S., 1999. *Neural Networks: A Comprehensive Foundation*. International edition. Prentice Hall. ISBN 9780132733502.

Hennemann, E., 1957. "Relation between size of neurons and their susceptibility to discharge". *Science*, Vol. 126, No. 126, pp. 1345–1347.

Ingram, J.N., Körding, K.P., Howard, I.S. and Wolpert, D.M., 2008. "The statistics of natural hand movements". *Experimental brain research*, Vol. 188, No. 2, pp. 223–236.

Klein, A.A., 2009. *A aplicação da fotogrametria para a coleta de dados da antropometria da mão*. Ph.D. thesis, Universidade Federal do Paraná.

Kosmashi, E.M., 2017. "Goniometry". URL `http://www.scranton.edu/faculty/kosmahl/courses/gonio/upper/pages/interpha-joint-flex.shtml`.

Perini, T.A., Oliveira, G.L.d., Ornellas, J.d.S. and Oliveira, F.P.d., 2005. "Cálculo do erro técnico de medição em antropometria". *Rev Bras Med Esporte*, Vol. 11, No. 1, pp. 81–5.

Rodriguez-Añez, C.R., 2001. "Anthropometry and it application in ergonomics". *Brazilian Journal of Kinanthropometry and Human Performance*, Vol. 3, No. 1, pp. 102–108.

Schmit, J., 2003. "human left hand". URL `https://grabcad.com/library/human-left-hand`.

Tymrak, B., Kreiger, M. and Pearce, J., 2014. "Mechanical properties of components fabricated with open-source 3-d printers under realistic environmental conditions". *Materials & Design*, Vol. 58, No. Supplement C, pp. 242 – 246.

Winter, D.A., 2009. *Biomechanics and motor control of human movement*. John Wiley & Sons, 4th edition.

9. RESPONSIBILITY NOTICE

The authors are the only responsible for the printed material included in this paper.